

Preparation of Neutrally Colorless, Transparent Polynorbornenes with Multiple Redox-Active Chromophores via Ring-Opening Metathesis Polymerization Toward Electrochromic Applications

WEI-REN LIAN,¹ KUN-LI WANG,² JYH-CHIANG JIANG,¹ DER-JANG LIAW,¹ KUEIR-RARN LEE,³ JUIN-YIH LAI³

¹Department of Chemical Engineering, National Taiwan University of Science and Technology, Taipei 10607, Taiwan

²Department of Chemical Engineering and Biotechnology, National Taipei University of Technology, Taipei 10608, Taiwan

³R&D Center for Membrane Technology, Department of Chemical Engineering, Chung Yuan University, Chung-Li 32023, Taiwan

Received 5 March 2011; accepted 30 April 2011

DOI: 10.1002/pola.24760

Published online 31 May 2011 in Wiley Online Library (wileyonlinelibrary.com).

ABSTRACT: A new electrochromic norbornene derivative containing triphenylamine groups (NBDTPAC8) was synthesized using norbornene amine and bromotriphenylamine. NBDTPAC8 was used in ring-opening metathesis polymerization to obtain poly(NBDTPAC8) using different Grubbs' catalysts and followed by hydrogen reduction to obtain poly(HNBDTPAC8). The glass transition temperatures (T_g) of poly(NBDTPAC8) and hydrogenated poly(HNBDTPAC8) were 132 and 89 °C, respectively. Poly(HNBDTPAC8) film exhibited a fluorescence maximum around 416 nm with a quantum yield of up to 60%. Hydrogenated poly(HNBDTPAC8) film showed excellent transparency (up to 93%). Poly(HNBDTPAC8) showed cyclic voltammetric and electrochromic behaviors similar to those of poly(NBDTPAC8). The cyclic voltammogram of a poly(HNBDTPAC8) film cast onto an indium

tin oxide (ITO)-coated glass substrate exhibited three reversible oxidation redox couples at 0.69, 0.94 and 1.38 V versus Ag/Ag⁺ in an acetonitrile solution. The electrochromic characteristics of poly(HNBDTPAC8) showed excellent stability and reversibility, with multi-staged color changes from its colorless neutral form to green, light blue and dark blue upon the application of potentials ranging from 0 to 1.60 V. The color switching time and bleaching time of the poly(HNBDTPAC8) film were 6.2 s and 4.3 s at 1175 nm and 6.6 s and 4.4 s at 970 nm, respectively. © 2011 Wiley Periodicals, Inc. *J Polym Sci Part A: Polym Chem* 49: 3248–3259, 2011

KEYWORDS: functionalization of polymers; redox polymers; ROMP; simulations; synthesis; transparency

INTRODUCTION Electrochromism (EC) results from the generation of different electronic absorption bands that correspond to changes between at least two states. In most cases, EC occurs by reduction–oxidation (redox) reactions.¹ Non-redox EC is also possible for some polarizable molecules that exhibit a spectroscopic shift on the application of a strong electric field, which is known as the Stark effect.² Devices that make use of electrochromic technology include smart windows,³ electrochromic displays,⁴ and electrochromic mirrors.⁵

The electrochromic effect occurs in many inorganic materials, such as transition metal oxides⁶ and mixed-valence metal complexes,⁷ as well as in organic materials, such as polyimides,^{8,9} polyamides,¹⁰ and conjugated polymers.^{11–14} Inorganic electrochromic materials suffer from processing and performance problems.¹⁵ For example, inorganic oxides typically require more than 60 s to switch states.¹⁶

Normally, most polyamides and polyimides have traditionally been difficult to process by spin coating because of their high glass transition temperatures and poor solubility in

organic solvents, which limit their widespread application.^{17,18} In addition, polyimides intrinsically exhibit color due to their strong charge transfer complex. Colored polymers are not preferred as electrochromic materials, and native color is one of the disadvantages for the practical use of these kinds of polymers in optical devices. Colorless electrochromic polymers are generally important, but their use is not common.^{19–21} A large difference in transmittance between colorless and colored states is desirable for electrochromic materials, because it provides high contrast.

On the other hand, it is well known that norbornene-based polymers are colorless, amorphous, and readily solution-processable polymers with high thermal stability and optical transparency.^{22–25} Ring-opening metathesis polymerization (ROMP) offers an effective way to polymerize norbornene monomers with different side chain substitutes.²⁶ Grubbs' ruthenium (Ru) carbene complexes efficiently catalyze ROMP under ambient conditions, with a high tolerance for polar functional groups.^{27–32} Thus, the use of a Ru-based catalyst in ROMP is a promising route to prepare polynorbornenes

Additional Supporting Information may be found in the online version of this article. Correspondence to: D.-J. Liaw (E-mail: liawdj@mail.ntust.edu.tw or liawdj@gmail.com or liawdj@ntu.edu.tw or liawdj@yahoo.com.tw)

Journal of Polymer Science Part A: Polymer Chemistry, Vol. 49, 3248–3259 (2011) © 2011 Wiley Periodicals, Inc.

with colorless, transparent, and easily solution-processable properties.

Triphenylamine (TPA) derivatives have shown excellent thermal, electrochemical stability, electron-donating ability, and optoelectronic properties.³³ They have been used as advanced materials for polymer memories,^{34–41} electroluminescence,⁴² chemosensor application,^{43,44} and electro-optical devices.⁴⁵ However, the oxidation of TPA may undergo the undesirable radical cation dimerization of the TPA moieties to produce tetraphenylbenzidine.⁴⁶ The addition of electron-donating substituents, such as an alkyl group at the para-position of the phenyl group of the TPA structure, could prevent coupling reactions and afford stable coloration.⁴⁷ Because of their noticeable change in coloration, TPA derivatives are regarded as good electrochromic materials.^{48–51} To the best of our knowledge, there has been no report about electrochromic materials based on polynorbornene derivatives with TPA pendant groups.

In this study, we prepared a colorless, transparent polynorbornene derivative containing electron-donating 2,4,4-trimethylpentan-2-yl substituted TPA with high molecular weights and low polydispersity indices via ROMP and then performed hydrogenation to afford saturated polynorbornene. The introduction of electron-donating 2,4,4-trimethylpentan-2-yl substituent is expected to prevent coupling reactions and lower the oxidation potentials/switching voltage.¹³ The basic properties of unsaturated polynorbornene and saturated polynorbornene, such as solubility, thermal properties, optical properties, electrochemical properties, and electrochromic properties, are discussed in this investigation.

EXPERIMENTAL

Materials

Dicyclopentadiene and allyl amine were purchased from Merck. Palladium acetate, sodium *tert*-butoxide, tri-*tert*-butylphosphine, and 1,4-dibromobenzene were purchased from Aldrich and used without further purification. Catalysts Ru (G1), Ru (G2), and Ru (G3) were obtained from Sigma-Aldrich, and 2,6-di-*tert*-butyl-4-methylphenol, *p*-toluenesulfonylhydrazide, and 1,1'-bis(diphenylphosphino)-ferrocene (DPPF) were purchased from Acros. The synthesis of 5-(amino methyl) bicyclo[2.2.1] hept-2-ene (NBMA, bp: 60–61 °C/11 mmHg) was accomplished via the Diels–Alder reaction of freshly cracked cyclopentadiene and allyl amine according to the published literature.^{52,53} Bis(4-(2,4,4-trimethylpentan-2-yl)phenyl)amine was purchased from OUCHI SHINKO and was recrystallized by ethanol (mp: 105–106 °C). The polymerization solvent, tetrahydrofuran (THF), was dried over sodium metal and distilled before use. Solvents such as xylene and benzene were purified by normal procedures and handled under a moisture-free atmosphere.

Measurements

High-resolution mass spectrum was recorded using a VG Platform Electrospray electronspray ionization (ESI)/MS apparatus in ESI mode. Weight-average (Mw) and number-average (Mn) molecular weights were determined by gel per-

meation chromatography (GPC). Five Waters (Ultrastryragel) columns 300 × 7.7 mm (guard, 500, 10³, 10⁴, and 10⁵ Å in a series) were used for GPC analysis with THF (1 mL min⁻¹) as an eluent. The eluents were monitored with a refractive index detector (RI 2000). Polystyrene was used as a standard. Cyclic voltammetry (CV) was performed with a CHI model 619A with indium tin oxide (ITO) used as a working electrode and a platinum wire as an auxiliary electrode at a scan rate of 50 mV s⁻¹ against an Ag/Ag⁺ reference electrode in a solution of 0.1 M tetrabutylammonium perchlorate (TBAP)/acetonitrile (CH₃CN). The spectroelectrochemical cell was composed of a 1-cm cuvette, ITO as a working electrode, a platinum wire as an auxiliary electrode, and a Ag/Ag⁺ reference electrode. The UV-vis spectra of the polymer films or solutions were recorded on a JASCO V-550 spectrophotometer at room temperature in air. Elemental analyses were performed on a PerkinElmer 2400 C, H, and N analyzer. ¹H and ¹³C NMR spectra were recorded on a Bruker DRX-500 instrument operating at 500 MHz for protons and 125 MHz for carbon. The melting temperature (*T*_m) and glass transition temperature (*T*_g) were measured on a DuPont 9000 differential scanning calorimeter (TA Instruments TA 910) at a heating rate of 10 °C min⁻¹ under a steady flow of nitrogen. Thermogravimetric data were obtained on a PerkinElmer TG/DTA (Diamond TG/DTA). Experiments were performed on 3–5-mg samples at a heating rate of 10 °C min⁻¹ under nitrogen- or air-flow conditions (20 cm³ min⁻¹).

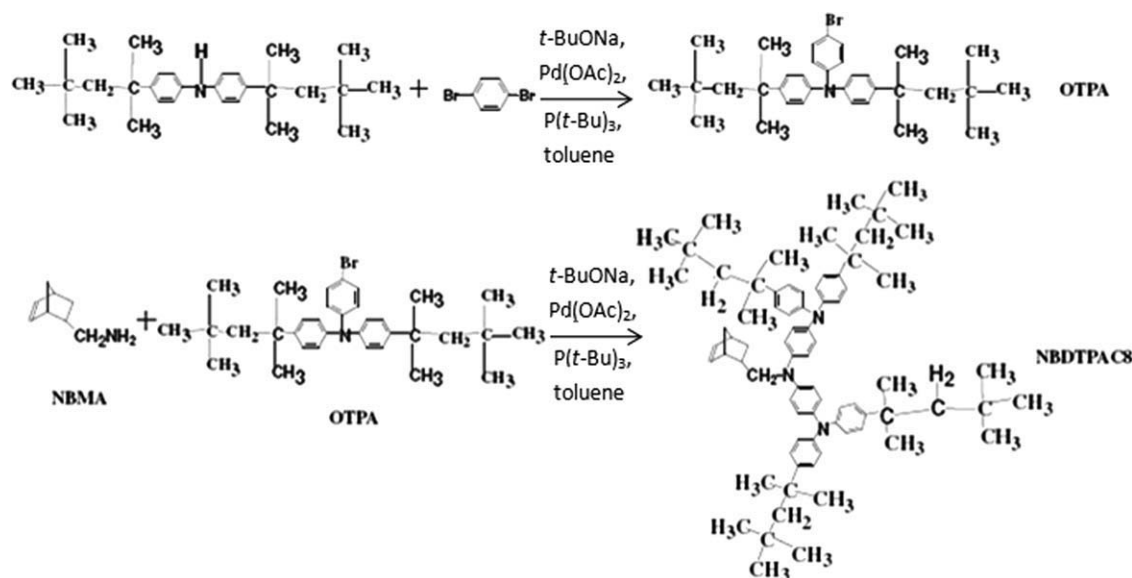
Synthesis of 4-Bromo-*N,N*-bis(4-(2,4,4-trimethylpentan-2-yl)phenyl)benzene-amine

Sodium *tert*-butoxide (8.2 g, 86 mmol), DPPF (0.27 g, 4.9 × 10⁻² mmol), dibromobenzene (8.7 g, 36 mmol), bis(4-(2,4,4-trimethylpentan-2-yl)phenyl)amine (9.4 g, 24 mmol), and palladium acetate (0.11 g, 4.8 × 10⁻¹ mmol) were dissolved in 100 mL of dry toluene. The mixture was heated, stirred at 120 °C for 7 h, and kept under a nitrogen atmosphere. Thereafter, the solvent was evaporated under reduced pressure. The product was purified by silica gel column chromatography by hexane and recrystallized from *n*-hexane to afford white crystals, 4-bromo-*N,N*-bis(4-(2,4,4-trimethylpentan-2-yl)phenyl)benzeneamine (Scheme 1, OTPA) at a 60% yield; mp 101–102 °C by DSC (10 °C min⁻¹). IR (KBr pellet, cm⁻¹): 3041 (C–H, aromatic stretching), 1045 (C–Br, aryl bromide).

¹H NMR (500 MHz, CDCl₃): δ (ppm) = 0.81 (s, 18H, H₁); 1.42 (s, 12H, H₃); 1.79 (s, 4H, H₂); 6.91–6.92 (d, *J* = 7.70 Hz, 2H, H₆); 6.98–7.00 (d, *J* = 7.13 Hz, 4H, H₅); 7.25–7.27 (d, *J* = 7.32 Hz, 4H, H₄); 7.29–7.31 (d, *J* = 7.50 Hz, 2H, H₇). ¹³C NMR (CDCl₃): (ppm) = 31.74 (C_e), 31.94 (C_a), 32.20 (C_b), 38.19 (C_d), 57.15 (C_c), 113.67 (C_j), 123.93 (C_h), 124.27 (C_k), 127.04 (C_g), 131.90 (C_i), 144.53 (C_i), 144.93 (C_f), 147.37 (C_m). ELEM ANAL. Calcd. for C₃₄H₄₆BrN : C, 74.43%; H, 8.45%; N, 2.55%. Found: C, 74.33%; H, 8.47%; N, 2.46%.

Synthesis of Norbornene Monomer with Triphenylamine Side Groups

Palladium acetate (4 mg, 2 × 10⁻² mmol), NBMA (0.16 g, 1.3 mmol), 4-bromo-*N,N*-bis(4-(2,4,4-trimethylpentan-2-yl)phenyl)benzenamine (Scheme 1, OTPA) (1.59 g, 2.90 mmol),



SCHEME 1 Synthesis of the norbornene monomer (NBDTPAC8) containing triphenylamine structures.

tri-*tert*-butylphosphine (10 mg, 4×10^{-2} mmol), and sodium *tert*-butoxide (0.78 g, 8 mmol) were dissolved in 100 mL of dry toluene. The reaction mixture was warmed to 110 °C for 5 h and kept under a nitrogen atmosphere. After the completion of the reaction, the solvent was removed under reduced pressure, and the residual was extracted with ether/water. The collected organic layer was dried over magnesium sulfate (MgSO_4) overnight and then filtered to remove MgSO_4 . After removing the solvent of the filtrate, the residue was purified by silica gel column chromatography (hexane) to obtain a white solid. Yields: 50%; mp: 120–122 °C by DSC ($10 \text{ }^\circ\text{C min}^{-1}$). IR (KBr pellet, cm^{-1}): 3040 (C–H, aromatic stretching), 1620 (C=C, cyclic alkene).

$^1\text{H NMR}$ (500 MHz, $\text{THF-}d_6$): δ (ppm) = 0.55–0.60 (t, $J = 7.11$ Hz, 1H, H_{n6n}), 0.68–0.80 (s, 72H, H_{15}), 1.23–1.35 (m, 5H, H_{x7s} , H_{x7a} , H_{n7s} , H_{n7a} , and H_{x6x}), 1.38–1.42 (m, 50H, H_{13} , H_{x5} , and H_{x6n}), 1.69–1.77 (s, 16H, H_{14}), 1.84–1.91 (t, $J = 7.33$ Hz, 1H, H_{n6x}), 2.52–2.61 (s, 1H, H_{n5}), 2.73–2.78 (s, 1H, H_{n1}), 2.77–2.88 (m, 3H, H_{x4} , H_{x1} , and H_{n4}), 3.34–3.47 (m, 2H, H_{n8}), 3.62–3.72 (m, 2H, H_{x8}), 5.72–5.74 (t, $J = 7.90$ Hz, 1H, H_{n2}), 6.07–6.08 (m, 2H, H_{x2} , and H_{x3}), 6.11–6.13 (t, $J = 7.85$ Hz, 1H, H_{n3}), 6.85–7.28 (m, 48H, H_{9-12}). $^{13}\text{C NMR}$ ($\text{THF-}d_6$): δ (ppm) = 25.50 (C_{13}), 27.88 (C_{x7}), 28.00 (C_{n7}), 30.76 (C_{20}), 31.08 (C_{21}), 31.19 (C_{x5}), 32.26 (C_{15}), 33.09 (C_{n6}), 38.85 (C_{n4}), 39.00 (C_{n5}), 43.02 (C_{x4}), 43.33 (C_{n1}), 46.01 (C_{x1}), 50.88 (C_{x6}), 57.98 (C_{n8}), 58.02 (C_{14}), 58.21 (C_{x8}), 122.60 (C_9), 123.80 (C_{11}), 126.00 (C_{10}), 127.92 (C_{12}), 133.85 (C_{n2}), 134.21 (C_{x2} and C_{x3}), 137.94 (C_{n3}) and 142.37, 144.31, 144.94 and 146.49 (C_{16} , C_{17} , C_{18} and C_{19}). ELEM ANAL. Calcd. for $\text{C}_{76}\text{H}_{103}\text{N}_3$: C, 86.22%; H, 9.81%; N, 3.97%. Found: C, 86.35%; H, 9.75%; N, 3.90%. High resolution electrospray ionization mass (HRESIMS): m/z 1058.8272 [$\text{M}+\text{H}$] $^+$ (calcd for $\text{C}_{76}\text{H}_{104}\text{N}_3^+$, 1058.8230, +3.59 ppm).

Synthesis of Poly(NBDTPAC8) Using Ring-Opening Metathesis Polymerization

The monomer, norbornene derivative containing triphenylamine groups (NBDTPAC8; 0.42 g, 0.4 mmol), was dissolved

in 4 mL of anhydrous THF and then degassed via freeze-pump-thaw cycles. A catalyst solution was prepared by dissolving Ru (G3) (0.3 mg, 4×10^{-4} mmol) in 0.5 mL of anhydrous THF in an argon-filled drybox. After degassing the monomer solution completely, the catalyst solution was injected into the monomer solution by a syringe. The polymerization was performed at 25 °C for 1 h. The reaction was terminated by the addition of a small amount of ethyl vinyl ether (0.2 mL). Poly(NBDTPAC8) was obtained by precipitation in excess methanol and was further purified by dissolving in benzene and reprecipitating in methanol. Poly(NBDTPAC8) dissolved in benzene was filtered, frozen, and dried. The yield of poly(NBDTPAC8) was 80%. The polymerizations of monomer NBDTPAC8 with the catalysts Ru (G1) and Ru (G2) were performed in the same manner. IR (KBr pellet, cm^{-1}): 1292 (C–N, aromatic amine), 1610 (C=C, cyclic alkene), 3036 (C–H, aromatic stretching).

$^1\text{H NMR}$ (500 MHz, $\text{THF-}d_6$): δ (ppm) = 0.64–3.17 (m, 7H, H_1 and H_{4-7}), 0.75–1.73 (m, 68H, H_{13-15}), 3.42–3.75 (d, 2H, $J = 8.65$ Hz, H_8), 5.31–5.42 (m, 2H, H_{2-3}), 6.79–7.14 (m, 24H, H_{9-12}). $^{13}\text{C NMR}$ ($\text{THF-}d_6$): δ (ppm) = 24.03 (C_{13}), 27.32–46.32 (C_1 , C_4 – C_7 , C_{15} , C_{20} , and C_{21}), 55.76 (C_8), 58.01 (C_{14}), 122.21–129.03 (C_{2-3} and C_9 – C_{12}), 142.32–146.78 (C_{16} – C_{19}). ANAL. Calcd. for $(\text{C}_{76}\text{H}_{103}\text{N}_3)_n$: C, 86.22%; H, 9.81%; N, 3.97%. Found: C, 86.55%; H, 9.65%; N, 3.80%.

Synthesis of Poly(HNBDTPAC8) Using Hydrogenated Agent

The polymer poly(NBDTPAC8) (1.26 g, 1.2 mmol) was dissolved in 8 mL of xylene in a Schlenk tube. To the above solution, 1.64 g (8.8 mmol) of hydrogenating agent, *p*-toluenesulfonhydrazide (7.3 equiv relative to the repeating unit), and a trace amount of 2,6-di-*tert*-butyl-4-methylphenol (inhibitor) were added. The polymer solution with hydrogenating agent was then degassed three times via a freeze-pump-thaw cycle and sealed. The solution was stirred at 120 °C for 12 h until the evolution of nitrogen stopped. The hydrogenated polymer poly(HNBDTPAC8) was obtained by precipitation in excess

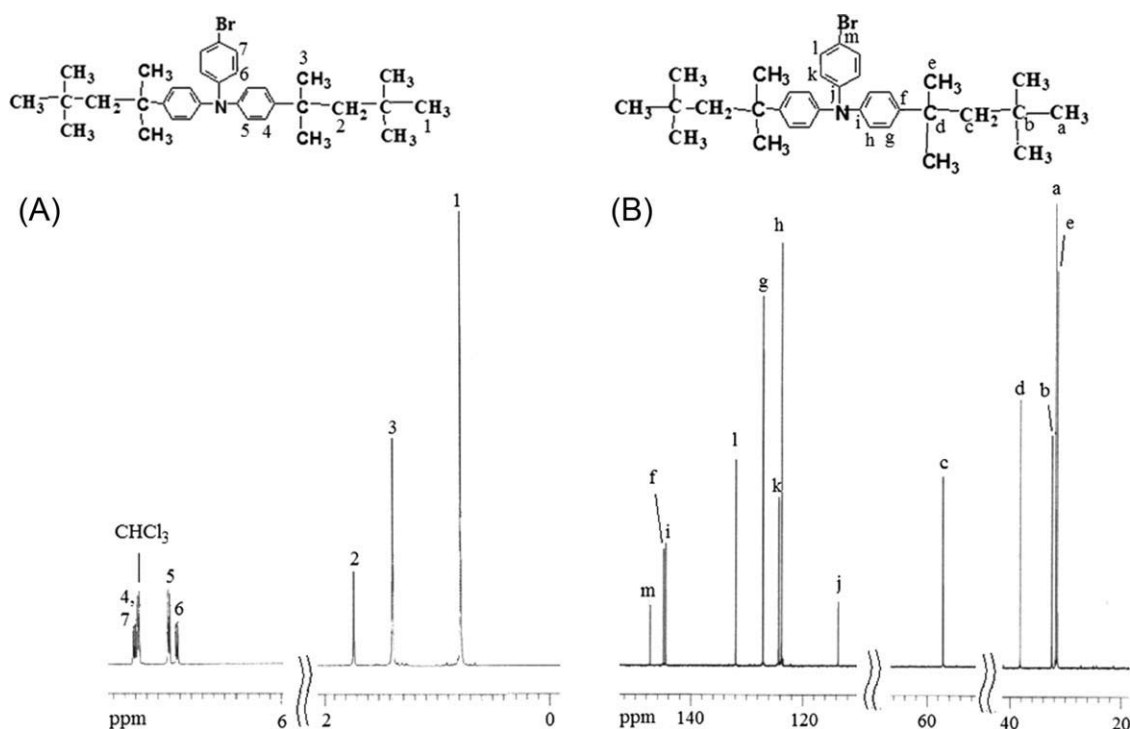


FIGURE 1 (A) ^1H NMR spectrum of OTPA (with CDCl_3 as the solvent) and (B) ^{13}C NMR spectrum of OTPA (with CDCl_3 as the solvent).

methanol and was further purified by dissolving in benzene and reprecipitating in methanol. Poly(HNBDTPAC8) dissolved in benzene was filtered, frozen, and dried. The yield of hydrogenated polymer poly(HNBDTPAC8) was 90%. IR (KBr pellet, cm^{-1}): 1282 (C—N, aromatic amine), 3040 (C—H, aromatic stretching).

^1H NMR (500 MHz, $\text{THF-}d_6$): δ (ppm) = 0.75–2.70 (m, 11H, H_{1-7}), 0.77–1.77 (m, 68H, H_{13-15}), 3.48–3.78 (d, 2H, $J = 8.75$ Hz, H_8), 6.74–7.37 (m, 24H, H_{9-12}). ^{13}C NMR ($\text{THF-}d_6$): δ (ppm) = 21.44–21.95 (C_2 and C_3), 26.12 (C_{13}), 30.23–43.11 (C_1 , C_4 – C_7 , C_{15} , C_{20} , and C_{21}), 54.73 (C_8), 58.04 (C_{14}), 127.76–131.21 (C_9 – C_{12}), 142.08–147.11 (C_{16} – C_{19}). ANAL. Calcd. for $(\text{C}_{76}\text{H}_{105}\text{N}_3)_n$: C, 86.06%; H, 9.98%; N, 3.96%. Found: C, 85.85%; H, 9.88%; N, 4.27%.

RESULTS AND DISCUSSION

Synthesis and Characterization

The norbornene derivative (NBDTPAC8) was successfully synthesized by the Buchwald–Hartwig reaction with 4-bromo-*N,N*-bis(4-(2,4,4-trimethylpentan-2-yl)phenyl)benzenamine (Scheme 1, OTPA) and 5-(amino methyl)bicyclo[2.2.1]hept-2-ene. The synthesis procedures of norbornene monomer (NBDTPAC8) containing TPA structures are outlined in Scheme 1. OTPA and NBDTPAC8 (Scheme 1) were characterized by elemental analysis, ^1H and ^{13}C NMR and two-dimensional NMR techniques. The ^1H NMR and ^{13}C NMR spectra of the OTPA and NBDTPAC8 are shown in the Figures 1 and 2, respectively. The ratio of NBDTPAC8 endoisomers and exoisomers was calculated to be 10:1 from the NMR spectrum

shown in Figure 2(A). Elemental analysis and the NMR spectra clearly confirm that the compounds OTPA and NBDTPAC8 are consistent with the proposed structures. The ROMP of NBDTPAC8 using different Grubbs' catalysts is shown in Scheme 2. The polymerization using different Grubbs' catalysts was performed for 1 h. After the polymerization was finished, the vinylic proton peaks of NBDTPAC8 at 5.70–6.13 ppm disappeared in the ^1H NMR spectrum of poly(NBDTPAC8), as shown in Figure 3(A). Then, new vinyl protons appeared as broad signals between 5.11 and 5.55 ppm due to the double bond in the polymer main chain. The *cis*/*trans* ratio of this polymer is roughly estimated to be 35/65 from the broad signals. The broad signal is due to the complicated overlap of vinylic protons of the *cis* and *trans* configurations in the ring-opened poly(NBDTPA). The ^{13}C NMR spectrum of poly(NBDTPAC8) is complex, with many overlapping multiple or broad unresolved peaks, and it is impossible to interpret them in terms of microstructural detail, as is often the case for polymers produced by ROMP.⁵⁴ In the ^{13}C NMR spectrum [Fig. 3(B)], the weak unresolved signals at 30–42 ppm are ascribed to the cyclic norbornene structure of the polymer. The weak unresolved signals are due to the possibility of head–tail additions and *cis*- and *trans*-vinylene forms. Poly(NBDTPAC8) was reduced using a hydrogenating agent to obtain poly(HNBDTPAC8). The ^1H and ^{13}C NMR spectra of poly(HNBDTPAC8) are shown in Figure 4. In Figure 4(A), the aromatic resonance signals of poly(HNBDTPAC8) between δ (ppm) 6.71 and 7.41 still appear, which indicates that the remaining TPA side groups and the resonance signals of olefinic protons of poly(NBDTPAC8) between δ (ppm) 5.11 and

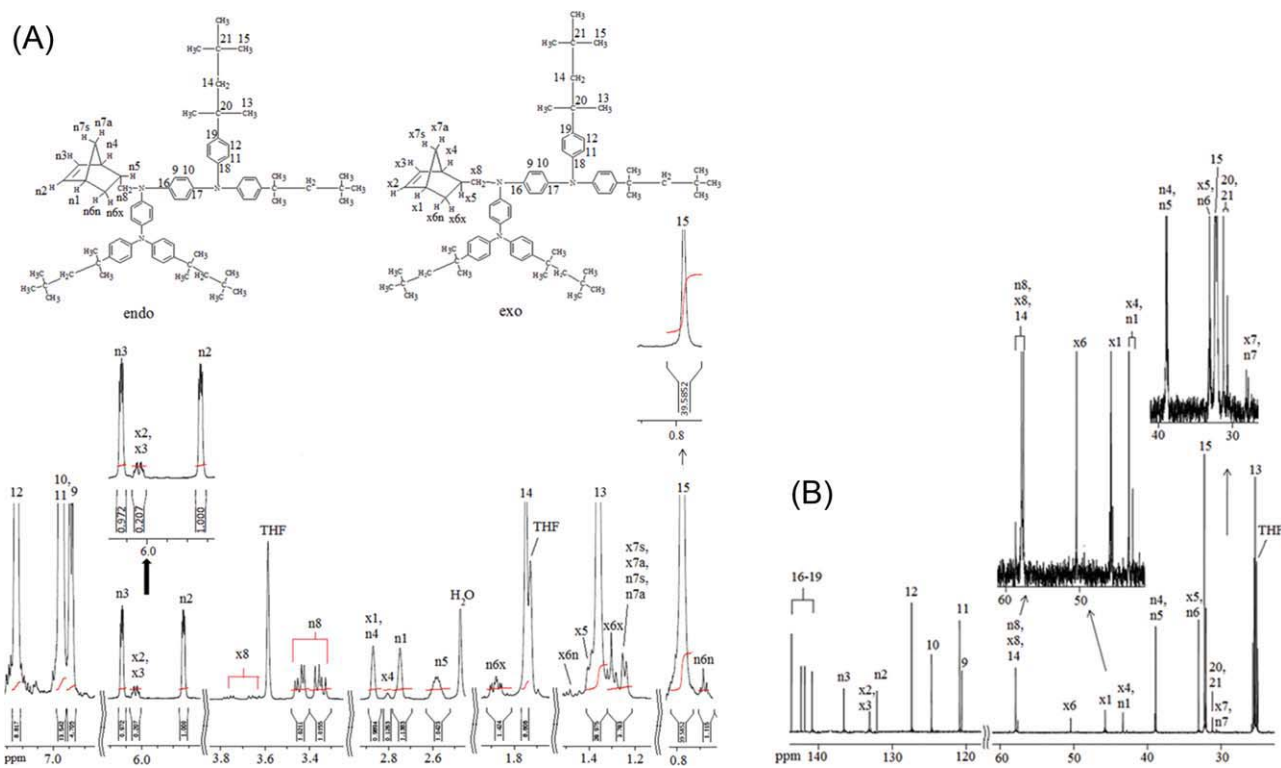
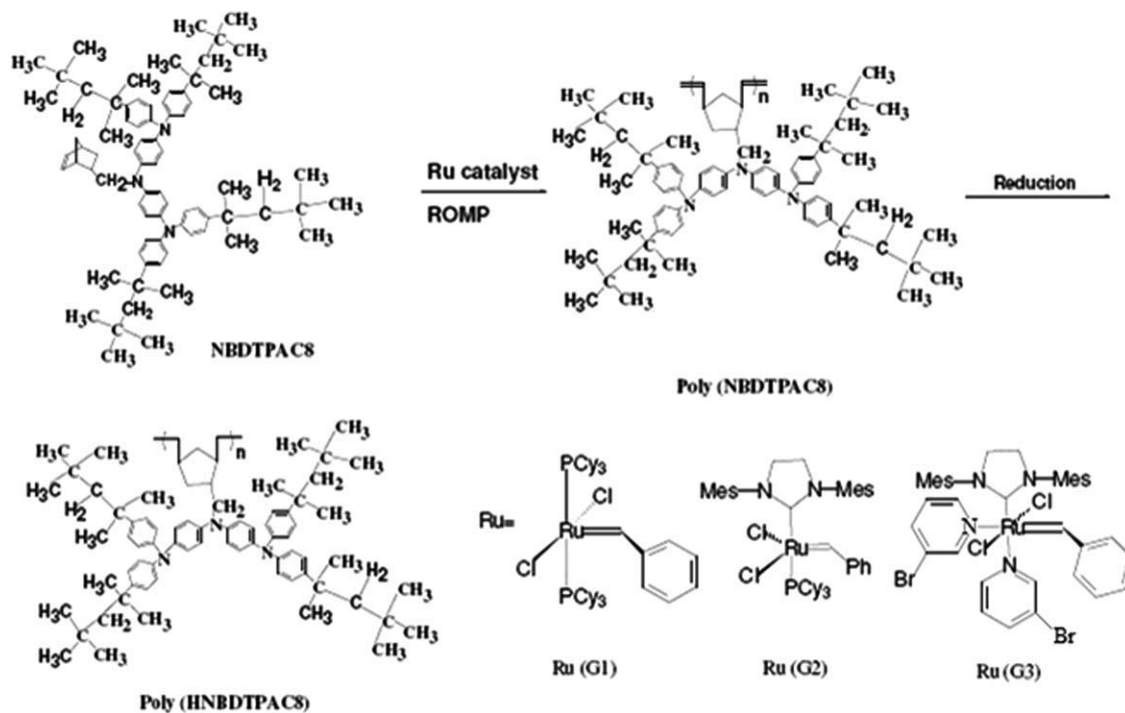


FIGURE 2 (A) ^1H NMR and (B) ^{13}C NMR spectra of NBDTPAC8 in $\text{THF-}d_8$. [Color figure can be viewed in the online issue, which is available at wileyonlinelibrary.com.]

5.55 disappear completely. The ^1H and ^{13}C NMR spectra of poly(HNBDTPAC8) are consistent with the proposed structure shown in Figure 4.

The ROMP of NBDTPAC8 using Ru (G1) was attempted but suffered from poor initiation and lower activity.⁵⁵ Ru (G2) exhibited good activity with respect to the polymerization of



SCHEME 2 Preparation of polynorbornenes, poly(NBDTPAC8), and poly(HNBDTPAC8).

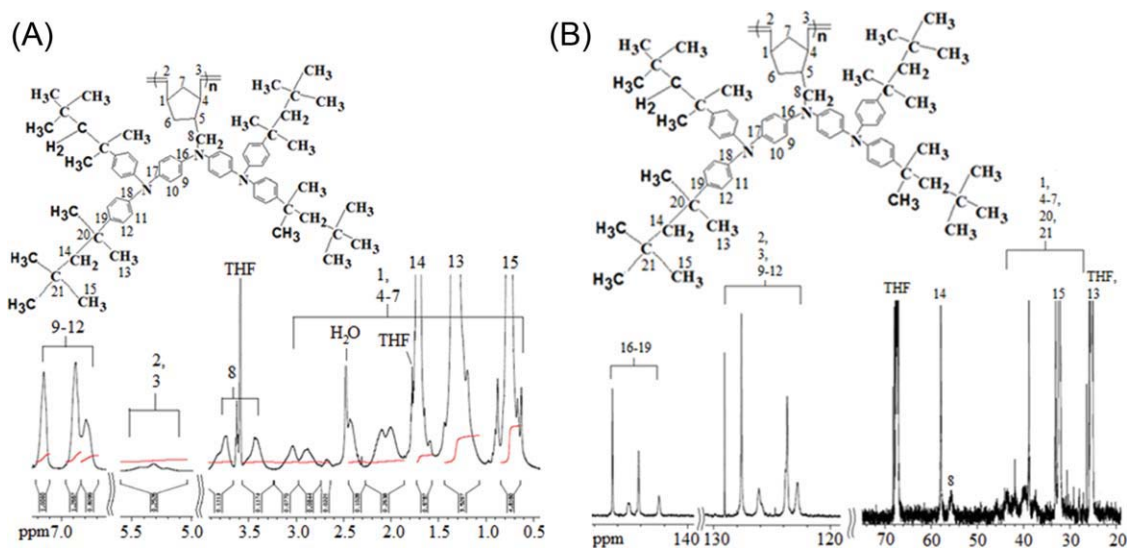


FIGURE 3 (A) ¹H NMR and (B) ¹³C NMR spectra of poly(NBDTPAC8) in THF-*d*₈. [Color figure can be viewed in the online issue, which is available at wileyonlinelibrary.com.]

NBDTPAC8, but the obtained polymer had an uncontrolled molecular weight and broad PDI due to slower initiation and faster propagation rates.⁵⁶ It is widely known that Ru (G3) exhibits better control due to faster initiation and inhibits side reactions such as back-biting.⁵⁷ We found that Ru (G3) promoted higher activity than Ru (G1) and Ru (G2). The polymerization of NBDTPAC8 by Grubbs' catalysts was performed in a nonliving fashion, as shown in Table 1. The molecular weight of the ring-opened polynorbornene was determined by GPC using polystyrene as the standard. The number-average molecular weights of poly(NBDTPAC8) obtained by Ru (G1), Ru (G2) and Ru (G3) were 0.66, 2.55, and 3.30×10^5 with yields of 15, 73, and 80%, respectively.

Basic Properties

Poly(NBDTPAC8) and poly(HNBDTPAC8) are both highly soluble in common organic solvents, such as toluene, xylene, benzene, chlorobenzene, and 1,2-dichlorobenzene, as well as in low boiling-point solvents, such as THF and ether, even in *n*-hexane at room temperature. However, they are insoluble in polar solvents, such as acetonitrile (CH₃CN), dimethyl sulfoxide (DMSO), *N,N*-dimethylacetamide, *N,N*-dimethylformamide, and *N*-methyl-2-pyrrolidinone, at room temperature. The excellent solubility in common organic solvents makes the hydrogenated ring-opened polynorbornene poly(HNBDTPAC8) a potential candidate for practical applications by spin-coating, dip-coating, or inject-printing processes to obtain thin films for optoelectronic devices. Poly(NBDTPAC8)

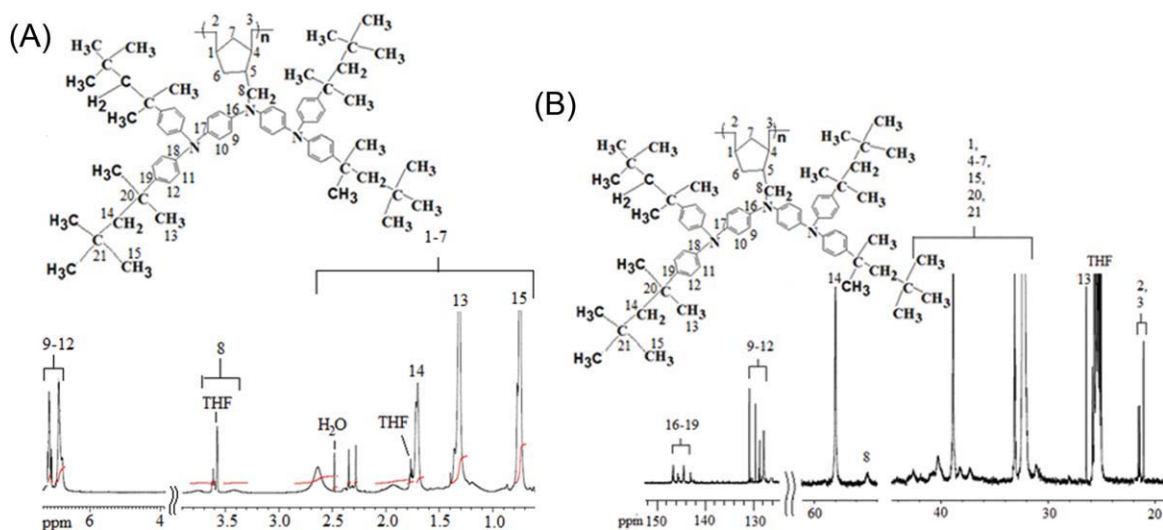


FIGURE 4 (A) ¹H NMR and (B) ¹³C NMR spectra of poly(HNBDTPAC8) in THF-*d*₈. [Color figure can be viewed in the online issue, which is available at wileyonlinelibrary.com.]

TABLE 1 The Molecular Weights and the Thermal Properties of Poly(NBDTPAC8) Polymerized by Ru (G1), Ru (G2), and Ru (G3)

Ru Catalyst	Yield ^a (%)	[M]/[I]	$M_{n(\text{GPC})} \times 10^{-5b}$	PDI ^b	T_g^c (°C)
Ru (G1)	15	1,000	0.66	1.35	135
Ru (G2)	73	1,000	2.55	1.68	132
Ru (G3)	80	1,000	3.30	1.33	132

^a Yield was determined gravimetrically.^b Determined by gel permeation chromatography (GPC) in THF using polystyrene as a standard.^c T_g was determined by DSC at a heating rate of 10 °C min⁻¹.

was not indefinitely stable in air atmosphere. When stored under ambient condition for weeks, poly(NBDTPAC8) became insoluble, whereas the poly(NBDTPAC8) stored under N₂ remained soluble. This is due to the oxidation and degradation of the unsaturated C=C double bonds in poly(NBDTPAC8).⁵⁸ Interestingly, the monomer NBDTPAC8, poly(NBDTPAC8), and poly(HNBDTPAC8) were soluble in chloroform at room temperature, but the color of the solution quickly changed to dark green under atmospheric conditions. However, when the samples were dissolved in chloroform and stored in the dark, the color of the samples remained unchanged. The ¹H NMR spectrum of the color-changed NBDTPAC8 in chloroform showed that the chemical shifts at 1.8~1.9, 2.5~2.6, 3.3~3.5, and 3.6~3.7 ppm disappeared, and 6.8~7.3 ppm became broader. This means that the newly prepared monomer and polymers are unstable in chloroform under light. We propose that these phenomena are related to carbon-chlorine single bond cleavages and the generation of free radicals, which interact with NBDTPAC8 under light.

The optical absorption and emission spectra of NBMA, NBDTPAC8, and poly(NBDTPAC8) were investigated by UV-vis and photoluminescence spectroscopy. In Figure 5(A), the UV-vis absorption of NBDTPAC8 and poly(NBDTPAC8) exhibit strong absorption at 311 and 315 nm (1×10^{-5} mol

L⁻¹; THF). However, there are no UV-vis absorption bands for NBMA at 250~350 nm (1×10^{-5} mol L⁻¹; THF). This means that the UV-vis absorption at 315 nm of poly(NBDTPAC8) can be ascribed to a π - π^* transition resulting from the conjugated TPA structure⁸ and is not related to the cyclic norbornene structure. The UV-vis absorption of poly(NBDTPAC8) in the solid state (thickness 3 μ m) also shows a similar absorbance peak with a slight red shift at 322 nm. This suggests the existence of interchain interactions in the solid-state polymer.¹² The optical absorption of poly(HNBDTPAC8) is similar to that of poly(NBDTPAC8). In Figure 5(B), the hydrogenated poly(HNBDTPAC8) film shows excellent transparency (up to 93%; thickness 3 μ m). The onset wavelength of solid-state poly(NBDTPAC8) observed from the UV-vis transmittance spectrum is approximately 390 nm, through which the energy gap of poly(NBDTPAC8) is estimated to be 3.2 eV.

Thermal Properties

The thermogravimetric behavior of poly(NBDTPAC8) and poly(HNBDTPAC8) obtained by Ru (G3) were tested. The thermogravimetric spectra of poly(NBDTPAC8) and hydrogenated poly(HNBDTPAC8) in nitrogen are shown in Figure 6. The unsaturated poly(NBDTPAC8) and saturated poly(HNBDTPAC8) showed 10% weight-loss temperatures ($T_{d10\%}$) at 374 and 418 °C under nitrogen, respectively. Under air, the unsaturated poly(NBDTPAC8) and saturated poly(HNBDTPAC8) showed 10% weight-loss temperatures ($T_{d10\%}$) at 366 and 407 °C, respectively. The saturated poly(HNBDTPAC8) is more stable than the unsaturated poly(NBDTPAC8), with a 10% increases in decomposition temperature to about 44 and 41 °C under nitrogen and air, respectively. In many applications, the instability of the unsaturated polymers with respect to thermal degradation is a concern.^{59,60} In Table 1, the polynorbornenes obtained by the three different Grubbs' ruthenium catalysts had glass transition temperatures (T_g) between 132 and 135 °C, and no remarkable difference was observed. The glass transition

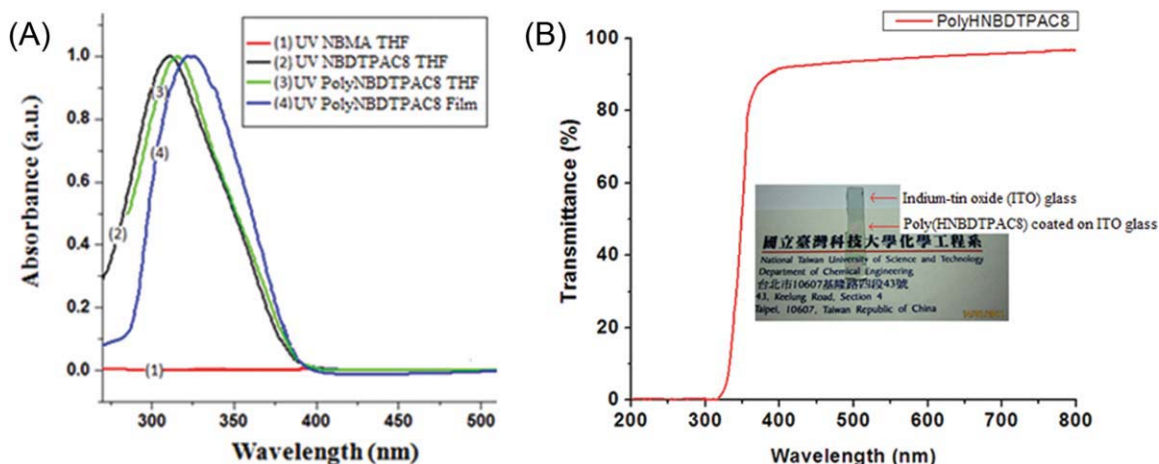


FIGURE 5 (A) Normalized UV-vis spectra of NBMA (1×10^{-5} mol L⁻¹; THF), NBDTPAC8 (1×10^{-5} mol L⁻¹; THF), poly(NBDTPAC8) (1×10^{-5} mol L⁻¹; THF) and poly(NBDTPAC8) film and (B) transparent spectra and film states of hydrogenated poly(HNBDTPAC8) (thickness 3 μ m). [Color figure can be viewed in the online issue, which is available at wileyonlinelibrary.com.]

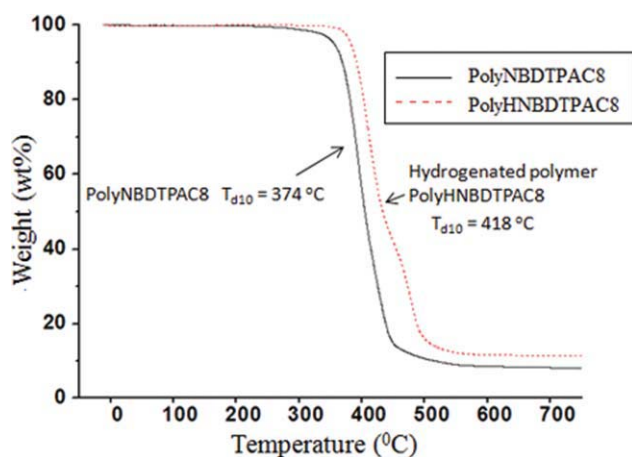


FIGURE 6 TGA curves for poly(NBDTPAC8) and hydrogenated poly(HNBDTPAC8) measured under nitrogen. Temperature was raised at a rate of $10\text{ }^{\circ}\text{C min}^{-1}$. [Color figure can be viewed in the online issue, which is available at [wileyonlinelibrary.com](#).]

temperatures (T_g) of poly(NBDTPAC8) and hydrogenated poly(HNBDTPAC8) were 132 and $89\text{ }^{\circ}\text{C}$, respectively. The prepared polynorbornenes have higher T_g s ($132\text{ }^{\circ}\text{C}$) than the polymers containing TPA moieties with a polynorbornene backbone ($23\text{--}120\text{ }^{\circ}\text{C}$).^{61,62} A decrease in T_g caused by hydrogenation was approximately $45\text{ }^{\circ}\text{C}$. The rotation around the hydrogenated carbon-carbon single bond clearly made the mobility of the polymer chain easier.⁶³

Electrochemical Properties

The electrochemical behaviors of poly(NBDTPAC8) and poly(HNBDTPAC8) were investigated by CV conducted on films cast on ITO-coated glass substrates as the working electrode in dry CH_3CN solution containing 0.1 M of TBAP as the electrolyte. The oxidative and reductive cycles of poly(NBDTPAC8) and poly(HNBDTPAC8) are shown in Figure 7. Poly

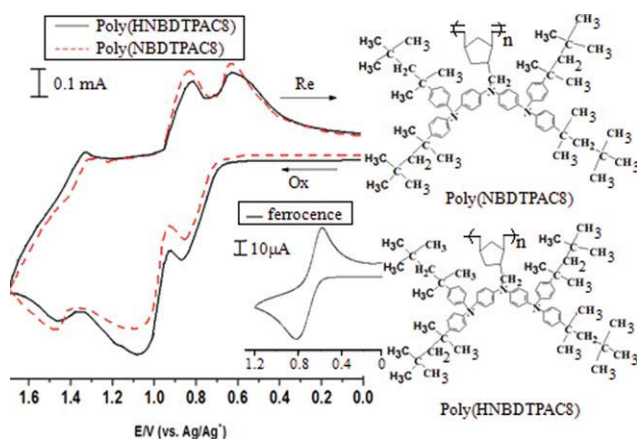


FIGURE 7 Cyclic voltammograms of poly(HNBDTPAC8) and poly(NBDTPAC8) in films cast on indium tin oxide (ITO)-coated glass substrates in CH_3CN containing 0.1 M TBAP. The scanning rate is 0.1 V s^{-1} . [Color figure can be viewed in the online issue, which is available at [wileyonlinelibrary.com](#).]

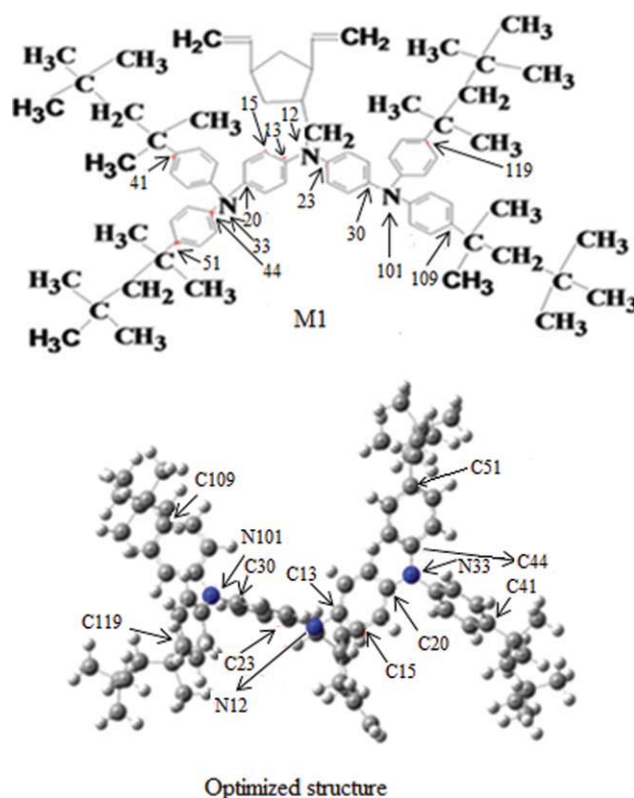


FIGURE 8 Sketch map of the studied structure (M1) and optimized structure determined by DFT/B3LYP/6-31G*. [Color figure can be viewed in the online issue, which is available at [wileyonlinelibrary.com](#).]

(NBDTPAC8) showed three reversible oxidation redox couples at $E_{1/2}$ values of 0.70, 0.93, and 1.39 V. Poly(HNBDTPAC8) showed three similar reversible oxidation redox couples at $E_{1/2}$ values of 0.69, 0.94, and 1.38 V. Both poly(NBDTPAC8) and poly(HNBDTPAC8) showed color changes from colorless to green, then to light blue, and finally to dark blue at applied potentials above 0.80, 1.15, and 1.50 V in the oxidative scan, respectively. From the oxidation potential relative to ferrocene/ferrocenium, which corresponds to -4.8 eV for ferrocene below the vacuum level,⁶⁴ we can approximately calculate the HOMO energy levels of poly(NBDTPAC8) and poly(HNBDTPAC8). The LUMO levels of poly(NBDTPAC8) and poly(HNBDTPAC8) were calculated according to the following equation: $\text{LUMO} = \text{HOMO} + E_g$. The HOMO and LUMO energy levels of poly(NBDTPAC8) are -4.75 and -1.59 eV , respectively. The electrochromic characteristics will be discussed below.

Theoretical Study of Oxidation Mechanism of Polynorbornene Derivatives

The electrochromic phenomenon is based on the redox behavior of a polymer; that is, it is based on the removal of electrons from the polymer and the capture of electrons by the polymer. We have reported the mechanism based on molecular orbital theory.^{8,10,11,14} The first electron is removed from the HOMO of the polymer to form a single occupied

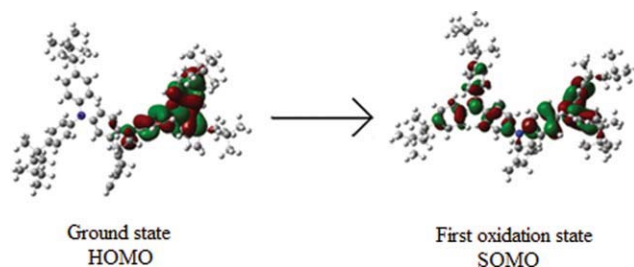
TABLE 2 Atomic Charge Distribution of Selected Atoms in Ground State, First Oxidation State, Second Oxidation State, Third Oxidation State, and the Charge Difference of $\Delta Q1$, $\Delta Q2$, and $\Delta Q3$ for M1

	G. S. ^a	Ox1 ^b	Ox2 ^c	Ox3 ^d	$\Delta Q1$ ^e	$\Delta Q2$ ^f	$\Delta Q3$ ^g
12 N	-0.4782	-0.3517	-0.3161	-0.3252	0.1266	0.0356	-0.0092
13 C	0.1687	0.1186	0.1595	0.2399	-0.0501	0.0409	0.0804
15 C	-0.2814	-0.2277	-0.2231	-0.2343	0.0537	0.0046	-0.0112
20 C	0.1128	0.1880	0.1981	0.1701	0.0752	0.0101	-0.0280
23 C	0.1121	0.1733	0.1834	0.1402	0.0612	0.0101	-0.0432
30 C	0.1599	0.1775	0.1956	0.1537	0.0175	0.0182	-0.0419
33 N	-0.4451	-0.3968	-0.3234	-0.2609	0.0482	0.0735	0.0625
41 C	-0.0432	-0.0073	0.0370	0.0997	0.0359	0.0443	0.0627
44 C	0.1555	0.1230	0.1167	0.1330	-0.0325	-0.0063	0.0164
51 C	-0.0503	-0.0099	0.0374	0.1026	0.0404	0.0473	0.0652
101 N	-0.4447	-0.3620	-0.3147	-0.2927	0.0827	0.0473	0.0220
109 C	-0.0343	0.0020	0.0431	0.0884	0.0363	0.0411	0.0452
119 C	-0.0351	0.0026	0.0447	0.0872	0.0377	0.0421	0.0425

^a G. S.: ground state.^b Ox1: losing one electron.^c Ox2: losing two electrons.^d Ox3: losing three electrons.^e $\Delta Q1$ = atomic charge difference of Ox1 and G. S.^f $\Delta Q2$ = atomic charge difference of Ox2 and Ox1.^g $\Delta Q3$ = atomic charge difference of Ox3 and Ox2.

molecular orbital (SOMO), and the second electron is removed from the SOMO to form the second oxidation state, and so on. All theoretical calculations in this study were performed using the quantum mechanical package Gaussian 03⁶⁵ based on the molecular orbital approach. The equilibrium structure of the polymers was determined using DFT with the B3LYP functional and the 6-31G* basis set. The studied model compound (M1) structure and structure optimized by B3LYP/6-31G* are plotted in Figure 8; the redox behavior of poly(NBDTPAC8) was selected for study. The electronic states of the neutral and oxidized structures of M1 were simulated, and the main results are summarized in Table 2 (see detailed distribution in Table S1 in the Supporting Information). The main atomic charge differences were located on the 12N, 13C, 15C, 20C, 23C, 30C, 33N, 41C, 44C, 51C, 101N, 109C, and 119C atoms. For the first oxidation (losing first electron), the 12N, 15C, 20C, 23C, 30C, 33N, 41C, 51C, 101N, 109C, and 119C atoms contributed 12.7, 5.4, 7.5, 6.1, 1.8, 4.8,

3.6, 4.0, 8.3, 3.6, and 3.8% of an electron, respectively, whereas the 13C and 44C received 5.0 and 3.3% of an electron. For the second oxidation, the 12N, 13C, 15C, 20C, 23C, 30C, 33N, 41C, 51C, 101N, 109C, and 119C atoms contributed 3.6, 4.1, 0.46, 1.0, 1.0, 1.8, 7.4, 4.4, 4.7, 4.7, 4.1, and 4.2% of an electron, respectively, whereas the 44C received 0.6% of an electron. For the third oxidation, the 13C, 33N, 41C, 44C, 51C, 101N, 109C, and 119C atoms contributed 8.0, 6.3, 6.3, 1.6, 6.5, 2.2, 4.5, and 4.2% of an electron, respectively, whereas the 12N, 15C, 20C, 23C, and 30C received 0.9, 1.1, 2.8, 4.3, and 4.2% of an electron. The electron density contours of the ground state and oxidation states are plotted by Gauss View in Figure 9, which illustrates the electron density distribution of the HOMO (ground state) and SOMO (first oxidized state) of the M1. The electron density distribution of the HOMO state is mainly located on the TPA moiety, and the HOMO-1 state has a similar electron density distribution to that of the HOMO state but located on the other TPA moiety. As for the SOMO state, the electron density distribution is mainly located on the di(triphenylamino)amine moiety. The model compound (M2) structure and optimized structure studied by B3LYP/6-31G* are plotted (see detailed data in the Supporting Information); these conditions were chosen to study the oxidative behavior of poly(HNBDTPAC8) at the molecular level. The oxidative behavior of poly(NBDTPAC8) is similar to that of poly(HNBDTPAC8). This suggests that the redox behaviors of poly(NBDTPAC8) and poly(HNBDTPAC8) are almost the same. The calculation results support the electrochemical experimental results.

**FIGURE 9** Electronic density contours of the frontier orbitals (M1) for optimized structure at ground state and first oxidation state. [Color figure can be viewed in the online issue, which is available at wileyonlinelibrary.com.]

Electrochromic Characteristics

For the electrochromic investigations, poly(NBDTPAC8) and poly(HNBDTPAC8) were cast onto ITO-coated glass slides, and a homemade electrochemical cell was built from a

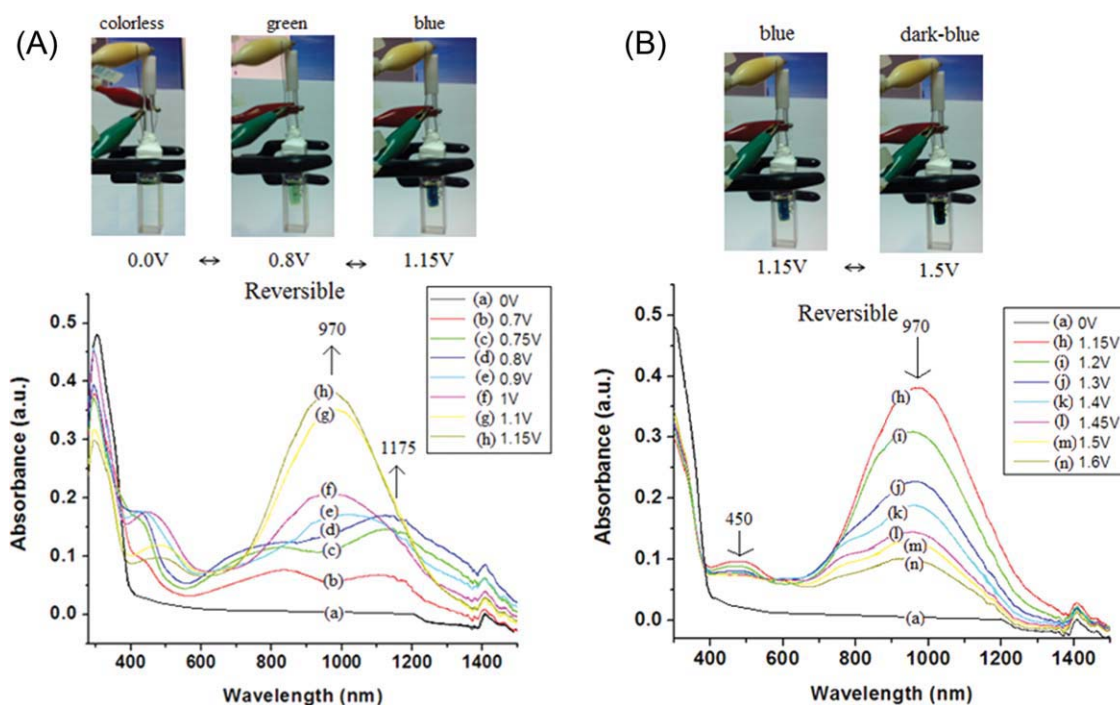


FIGURE 10 Absorption spectral change of poly(NBDTPAC8) thin film (in CH_3CN with 0.1 M TBAP as the supporting electrolyte) (A) Eappl: (a) 0.00, (b) 0.70, (c) 0.75, (d) 0.80, (e) 0.90, (f) 1.00, (g) 1.10, and (h) 1.15 V. (B) Eappl: (a) 0.00, (h) 1.15, (i) 1.20, (j) 1.30, (k) 1.40, (l) 1.45, (m) 1.50, and (n) 1.60 V.

commercial UV-visible cuvette. The cell was placed in the optical path of the sample light beam in a UV-vis-NIR spectrophotometer, which allowed us to acquire electronic absorption spectra *in situ* under potential control in a 0.1 M TBAP/ CH_3CN solution. The results for the poly(NBDTPAC8) film (thickness about 3 μm) are presented in Figure 10 as a

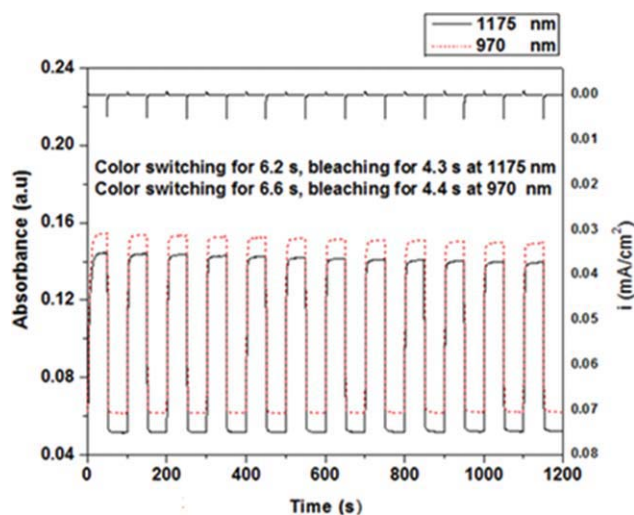


FIGURE 11 Current consumption and potential step absorptometry of poly(NBDTPAC8) (in CH_3CN with 0.1 M TBAP as the supporting electrolyte) by applying a potential step (0.00–0.80 V). [Color figure can be viewed in the online issue, which is available at wileyonlinelibrary.com.]

series of UV-vis-NIR absorbance curves correlated to electrode potentials. When the applied potentials were increased positively from 0 to 0.80 V [Fig. 10(A)], the new bands rose at 970 and 1175 nm due to the first oxidation. When the potential was increased to 1.15 V, corresponding to the second oxidation step, the peak at 970 nm still increased, and another peak at 1175 nm disappeared. Meanwhile, the film changed from its neutral colorless state to green and then to a light blue as shown in Figure 10(A) due to the oxidations. By applying an even more positive potential bias up to 1.50 V, corresponding to the third oxidation step as shown in Figure 10(B), the peak at 970 nm gradually decreased in intensity and the peak at 450 nm decreased. As the oxidation continued, the poly(NBDTPAC8) film continued to exhibit a color change from light blue to dark blue. The observed UV-vis-NIR absorption changes in the poly(NBDTPAC8) film at various potentials are fully reversible and are associated with strong color changes. The poly(HNBDTPAC8) film showed similar spectral changes. For electrochromic switching studies, polymer films were cast onto ITO-coated glass slides in the same manner as that described above. Although the films were switched, the absorbance at the given wavelength was monitored as a function of time by UV-vis-NIR spectroscopy. The switching data for poly(NBDTPAC8) are shown in Figure 11. The switching time was calculated at 90% of the full switch because of the difficulty in perceiving any further color changes with the naked eye beyond this point. The thin poly(NBDTPAC8) film at 0.80 V required 6.2 s to switch and 4.3 s to bleach at 1175 nm. At 970 nm, the thin poly(NBDTPAC8) film at 0.80 V required 6.6 s to switch and

4.4 s to bleach. Poly(HNBDTPAC8) showed electrochromic stability similar to that of poly(NBDTPAC8). Over continuous cyclic scans between 0.00 and 0.80 V, the poly(NBDTPAC8) and poly(HNBDTPAC8) films exhibited good electrochromic stability.

CONCLUSIONS

A new class of electrochromic polymer based on polynorbornenes containing electroactive chromophores was designed and prepared via ROMP to obtain poly(NBDTPAC8) and was followed by hydrogenation to obtain poly(HNBDTPAC8). Poly(NBDTPAC8) and hydrogenated poly(HNBDTPAC8) exhibited similar electrochemical and electrochromic behaviors with high contrast and electrochromic reversibility. Poly(HNBDTPAC8) shows greater thermal stability than poly(NBDTPAC8) does, whereas poly(NBDTPAC8) exhibits a higher glass transition temperature than does poly(HNBDTPAC8). Both polynorbornenes are colorless and transparent in their neutral state and exhibit higher glass transition temperatures than do general polynorbornenes. These excellent characteristics suggest that the prepared colorless polynorbornenes are good candidates for electrochromic materials.

The authors thank the National Science Council of the Republic of China for the financial support for this work. The HRESIMS spectrum was obtained at instrument centers of National Taiwan University. The assistances of the Shou-ling Huang and Shu-Yun Sun are gratefully appreciated.

REFERENCES AND NOTES

- Tu, X.; Fu, X.; Jiang, Q.; Liu, Z.; Chen, G. *Dyes Pigments* 2011, 88, 39–43.
- Cho, M. *J Chem Phys* 2009, 130, 094505.
- Gillaspie, D. T.; Tenent, R. C.; Dillon, A. C. *J Mater Chem* 2010, 20, 9585–9592.
- Balan, A.; Baran, D.; Toppare, L. *J Mater Chem* 2010, 20, 9861–9866.
- Tajima, K.; Yamada, Y.; Okada, M.; Yoshimura, K. *Thin Solid Films* 2010, 519, 934–937.
- Sequeira, C. A. C.; Santos, D. M. F. *J Electrochem Soc* 2010, 157, J202–J207.
- Mortimer, R. J.; Reynolds, J. R. *J Mater Chem* 2005, 15, 2226–2233.
- Chang, C. H.; Wang, K. L.; Jiang, J. C.; Liaw, D. J.; Lee, K. R.; Lai, J. Y.; Lai, K. H. *Polymer* 2010, 51, 4493–4502.
- Wang, K. L.; Liu, Y. L.; Shih, I. H.; Neoh, K. G.; Kang, E. T. *J Polym Sci Part A: Polym Chem* 2010, 48, 5790–5800.
- Chang, C. H.; Wang, K. L.; Jiang, J. C.; Liaw, D. J.; Lee, K. R.; Lai, J. Y.; Chiu, K. Y.; Su, Y. O. *J Polym Sci Part A: Polym Chem* 2010, 48, 5659–5669.
- Wu, H. Y.; Wang, K. L.; Jiang, J. C.; Liaw, D. J.; Lee, K. R.; Lai, J. Y.; Chen, C. L. *J Polym Sci Part A: Polym Chem* 2010, 48, 3913–3923.
- Wu, H. Y.; Wang, K. L.; Liaw, D. J.; Lee, K. R.; Lai, J. Y. *J Polym Sci Part A: Polym Chem* 2010, 48, 1469–1476.
- Chen, W. H.; Wang, K. L.; Liaw, D. J.; Lee, K. R.; Lai, J. Y. *Macromolecules* 2010, 43, 2236–2243.
- Chen, W. H.; Wang, K. L.; Hung, W. Y.; Jiang, J. C.; Liaw, D. J.; Lee, K. R.; Lai, J. Y.; Chen, C. L. *J Polym Sci Part A: Polym Chem* 2010, 48, 4654–4667.
- Yuan, Y. F.; Xia, X. H.; Wu, J. B.; Gui, J. S.; Chen, Y. B.; Guo, S. Y. *J Membrane Sci* 2010, 364, 298–303.
- Park, Y. T.; Grunlan, J. C. *Electrochim Acta* 2010, 55, 3257–3267.
- Yang, H. H. *Aromatic High-Strength Fibers*; Wiley, New York, 1989.
- Imai, Y. *High Perform Polym* 1995, 7, 337–345.
- Tajima, K.; Yamada, Y.; Bao, S.; Okada, M.; Yoshimura, K. *Appl Phys Express* 2008, 1, 0670071–0670073.
- Tajima, K.; Yamada, Y.; Bao, S.; Okada, M.; Yoshimura, K. *J Appl Phys* 2008, 103, 013512.
- Bao, S.; Tajima, K.; Yamada, Y.; Okada, M.; Yoshimura, K. *Applied Physics A: Materials Science and Processing* 2007, 87, 621–624.
- Yang, D.; Huang, W.; Yu, J.; Jiang, J.; Zhang, L.; Xie, M. *Polymer* 2010, 51, 5100–5106.
- Feng, K.; Zuniga, C.; Zhang, Y. D.; Kim, D.; Barlow, S.; Marder, S. R.; Brédas, J. L.; Weck, M. *Macromolecules* 2009, 42, 6855–6864.
- http://www.jsr.co.jp/jsr_e/pd/op/arton-pop02.html. Accessed on May 17, 2011.
- K. Goto, J. Private Communication (2009) Tokyo.
- Ye, Q.; Wang, X.; Li, S.; Zhou, F. *Macromolecules* 2010, 43, 5554–5560.
- Santiago, A. A.; Vargas, J.; Fomine, S.; Gaviño, R.; Tlenkopatchev, M. A. *J Polym Sci Part A: Polym Chem* 2010, 48, 2925–2933.
- Kreutzwiesner, E.; Noormofidi, N.; Wiesbrock, F.; Kern, W.; Rametsteiner, K.; Stelzer, F.; Slugovc, C. *J Polym Sci Part A: Polym Chem* 2010, 48, 4504–4514.
- Choi, M. C.; Hwang, J. C.; Kim, C.; Kim, Y.; Ha, C. S. *J Polym Sci Part A: Polym Chem* 2010, 48, 5189–5197.
- Kurzahls, S.; Binder, W. H. *J Polym Sci Part A: Polym Chem* 2010, 48, 5522–5532.
- Sutthasupa, S.; Shiotsuki, M.; Matsuoka, H.; Masuda, T.; Sanda, F. *Macromolecules* 2010, 43, 1815–1822.
- Grubbs, R. H. *Handbook of Metathesis*; Wiley-VCH, Germany 2003, 3, 79–111.
- Li, B.; Li, Q.; Liu, B.; Yue, Y.; Yu, M. *Dyes Pigments* 2011, 88, 301–306.
- Ling, Q. D.; Chang, F. C.; Song, Y.; Zhu, C. X.; Liaw, D. J.; Chan, D. S. H.; Kang, E. T.; Neoh, K. G. *J Am Chem Soc* 2006, 128, 8732–8733.
- Ling, Q. D.; Liaw, D. J.; Zhu, C.; Chan, D. S. H.; Kang, E. T.; Neoh, K. G. *Prog Polym Sci* 2008, 33, 917–978.
- Ling, Q. D.; Liaw, D. J.; Teo, E. Y. H.; Zhu, C.; Chan, D. S. H.; Kang, E. T.; Neoh, K. G. *Polymer* 2007, 48, 5182–5201.

- 37** Zhuang, X. D.; Chen, Y.; Li, B. X.; Ma, D. G.; Zhang, B.; Li, Y. *Chem Mater* 2010, 22, 4455–4461.
- 38** Wang, K. L.; Liu, Y. L.; Lee, J. W.; Neoh, K. G.; Kang, E. T. *Macromolecules* 2010, 43, 7159–7164.
- 39** Liu, Y. L.; Wang, K. L.; Huang, G. S.; Zhu, C. X.; Tok, E. S.; Neoh, K. G.; Kang, E. T. *Chem Mater* 2009, 21, 3391–3399.
- 40** Liu, Y. L.; Ling, Q. D.; Kang, E. T.; Neoh, K. G.; Liaw, D. J.; Wang, K. L.; Liou, W. T.; Zhu, C. X.; Chan, D. S. H. *J Appl Phys* 2009, 105, 044501.
- 41** Wang, K. L.; Tseng, T. Y.; Tsai, H. L.; Wu, S. C. *J Polym Sci Part A: Polym Chem* 2008, 46, 6861–6871.
- 42** Huang, S. T.; Liaw, D. J.; Hsieh, L. G.; Chang, C. C.; Leung, M. K.; Wang, K. L.; Chen, W. T.; Lee, K. R.; Lai, J. Y.; Chan, L. H.; Chen, C. T. *J Polym Sci Part A: Polym Chem* 2009, 47, 6231–6245.
- 43** Wang, K. L.; Liou, W. T.; Liaw, D. J.; Chen, W. T. *Dyes Pigments* 2008, 78, 93–100.
- 44** Wang, K. L.; Liou, W. T.; Liaw, D. J.; Huang, S. T. *Polymer* 2008, 49, 1538–1546.
- 45** Wang, K. L.; Huang, S. T.; Hsieh, L. G.; Huang, G. S. *Polymer* 2008, 49, 4087–4093.
- 46** Leung, M. K.; Chou, M. Y.; Su, Y. O.; Chiang, C. L.; Chen, H. L.; Yang, C. F.; Yang, C. C.; Lin, C. C.; Chen, H. T. *Org Lett* 2003, 5, 839–842.
- 47** Ito, A.; Ino, H.; Tanaka, K.; Kanemoto, K.; Kato, T. *J Org Chem* 2002, 67, 491–498.
- 48** Beaupré, S.; Dumas, J.; Leclerc, M. *Chem Mater* 2006, 18, 4011–4018.
- 49** Choi, K.; Yoo, S. J.; Sung, Y. E.; Zentel, R. *Chem Mater* 2006, 18, 5823–5825.
- 50** Otero, L.; Sereno, L.; Fungo, F.; Liao, Y. L.; Lin, C. Y.; Wong, K. T. *Chem Mater* 2006, 18, 3495–3502.
- 51** Natera, J.; Otero, L.; Sereno, L.; Fungo, F.; Wang, N. S.; Tsai, Y. M.; Hwu, T. Y.; Wong, K. T. *Macromolecules* 2007, 40, 4456–4463.
- 52** Liaw, D. J.; Chen, T. P.; Huang, C. C. *Macromolecules* 2005, 38, 3533–3538.
- 53** Liaw, D. J.; Tsai, J. S.; Wu, P. L. *Macromolecules* 2000, 33, 6925–6929.
- 54** Liaw, D. J.; Huang, C. C.; Hong, S. M. *J Polym Sci Part A: Polym Chem* 2006, 44, 6287–6298.
- 55** Nishihara, Y.; Inoue, Y.; Nakayama, Y.; Shiono, T.; Takagi, K. *Macromolecules* 2006, 39, 7458–7460.
- 56** Nishihara, Y.; Izawa, S.; Inoue, Y.; Nakayama, Y.; Shiono, T.; Takagi, K. *J Polym Sci Part A: Polym Chem* 2008, 46, 3314–3325.
- 57** Nishihara, Y.; Doi, Y.; Izawa, S.; Li, H. Y.; Inoue, Y.; Kojima, M.; Chen, J. T.; Takagi, K. *J Polym Sci Part A: Polym Chem* 2010, 48, 485–491.
- 58** Delaude, L.; Demonceau, A.; Noels, A. F. *Macromolecules* 1999, 32, 2091–2103.
- 59** Sohn, B. H.; Gratt, J. A.; Lee, J. K.; Cohen, R. E. *J Appl Polym Sci* 1995, 58, 1041–1046.
- 60** Kodemura, J.; Natsuume, T. *Polym J* 1995, 27, 1167–1172.
- 61** Hreha, R. D.; Haldi, A.; Domercq, B.; Barlow, S.; Kippelen, B.; Marder, S. R. *Tetrahedron* 2004, 60, 7169–7176.
- 62** Bellmann, E.; Shaheen, S. E.; Thayumanavan, S.; Barlow, S.; Grubbs, R. H.; Marder, S. R.; Kippelen, B.; Peyghambarian, N. *Chem Mater* 1998, 10, 1668–1676.
- 63** Yoshida, Y.; Goto, K.; Komiya, Z. *J Appl Polym Sci* 1997, 66, 367–375.
- 64** Grazulevicius, J. V.; Stroehriegl, P.; Pielichowski, J.; Pielichowski, K. *Prog Polym Sci* 2003, 28, 1297–1353.
- 65** Frisch, M. J. T.; G. W.; Schlegel, H. B.; Scuseria, G. E.; Robb, M. A.; Cheeseman, J. R.; Montgomery, J. A.; Vreven, T., Jr.; Kudin, K. N.; Burant, J. C.; Millam, J. M.; Iyengar, S. S.; Tomasi, J.; Barone, V.; Mennucci, B.; Cossi, M.; Scalmani, G.; Rega, N.; Petersson, G. A.; Nakatsuji, H.; Hada, M.; Ehara, M.; Toyota, K.; Fukuda, R.; Hasegawa, J.; Ishida, M.; Nakajima, T.; Honda, Y.; Kitao, O.; Nakai, H.; Klene, M.; Li, X.; Knox, J. E.; Hratchian, H. P.; Cross, J. B.; Adamo, C.; Jaramillo, J.; Gomperts, R.; Stratmann, R. E.; Yazyev, O.; Austin, A. J.; Cammi, R.; Pomelli, C.; Ochterski, J. W.; Ayala, P. Y.; Morokuma, K.; Voth, G. A.; Salvador, P.; Dannenberg, J. J.; Zakrzewski, V. G.; Dapprich, S.; Daniels, A. D.; Strain, M. C.; Farkas, O.; Malick, D. K.; Rabuck, A. D.; Raghavachari, K.; Foresman, J. B.; Ortiz, J. V.; Cui, Q.; Baboul, A. G.; Clifford, S.; Cioslowski, J.; Stefanov, B. B.; Liu, G.; Liashenko, A.; Piskorz, P.; Komaromi, I.; Martin, R. L.; Fox, D. J.; Keith, T.; Al-Laham, M. A.; Peng, C. Y.; Nanayakkara, A.; Challacombe, M.; Gill, P. M. W.; Johnson, B.; Chen, W.; Wong, M. W.; Gonzalez, C.; Pople, J. A. *Gaussian 03, Revision D.02*; Gaussian, Inc.: Wallingford, CT, 2004.